2.2 Properties of the Top Quark

The top quark, with mass ~ 175 GeV/c^2, is strongly coupled to the electroweak symmetry breaking mechanism, and decays to a real W and a b-quark before hadronizing. A program to characterize the properties of this unconventional fermion is an obvious scientific priority. The accessibility of the top quark at the Fermilab Tevatron, in conjunction with the planned luminosity and detector upgrades for Run II, creates a new arena for experimental particle physics at an existing facility, and we should fully exploit this unique opportunity over the next decade.

Tevatron Run I brought the discovery of the top quark, the first direct measurements of its mass and cross section [2, 3, 4], and valuable first experience in top quark physics. We established techniques to identify b-quark jets using secondary vertices and soft leptons from the decays $B \to \ell\nu X$, and the essential utility of b-tagging in the isolation of the top signal and the reconstruction of the final state. We established techniques for the accurate measurement of the mass and decay kinematics of a heavy object in final states with jets, and the essential utility of *in situ* jet calibration techniques. We have begun to explore a variety of other measurements, all of them presently limited by statistics.

Armed with this experience, we have considered the program of Top Quark Physics accessible at CDF II with 2 fb^{-1}at the Tevatron [1]. Our study differs from the usual "future program" proposal by being grounded in a well understood detector in a well studied environment. We will show that the CDF II detector will be capable of a complete characterization of the main properties of the top quark, and we will establish the probable precisions that can be achieved using 2 fb^{-1}of Tevatron collider data.

We begin here by reviewing the top analysis results of Run I. Next, we discuss the impact of the detector upgrade components on the top physics of Run II. Finally we describe the Run II top physics program, including yields, the mass measurement, production properties, branching ratios, and decays.

2.2.1 Review of Run I Analysis

Using 19.3 pb^{-1} from Run Ia, CDF presented initial evidence for the top quark in the spring of 1994 [2]. A year later, with an additional 48 pb^{-1} from Run Ib, CDF confirmed its original evidence for the top quark[3]. We describe below the isolation of the signal in several different decay modes and the measurements made with these first small samples.

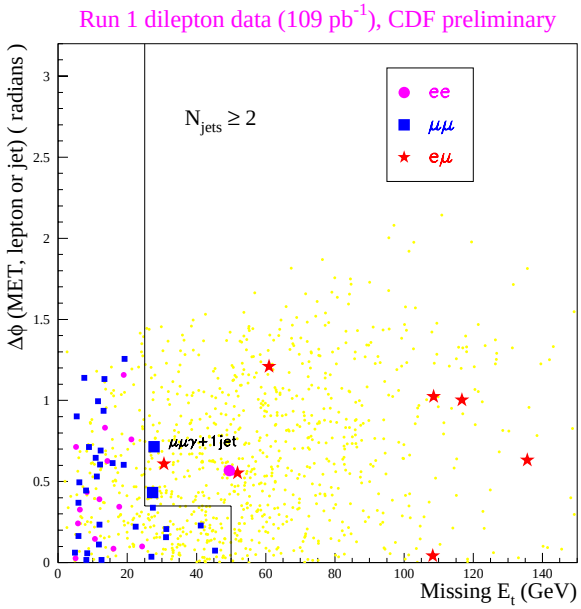

Figure 2.1: $\Delta\phi$ vs. $\not\!\!E_T$ in the dilepton sample. The small grey dots are the result of a $t\bar{t}$ Monte Carlo simulation with $m_{top} = 175$ GeV/c^2.

2.2.1.1 Dilepton Mode

In the standard model, the t and $\bar{t}$-quarks both decay almost exclusively to a W-boson and a b-quark. In the "dilepton" channel, both W's decay leptonically ($W \to \ell\nu$), and we search for leptonic W decays to an electron or a muon. The nominal signature in this channel is two high-P_T leptons, missing transverse energy (from the two ν's), and two jets from the b-quarks. Acceptance for this channel is small, mostly due to the product branching ratio of both W's decaying leptonically (only about 5%). In the 110 pb^{-1} from Run I, CDF observed 7 $e\mu$ events, 2 $\mu\mu$ events, and 1 ee event. Figure 2.1 shows the 10 candidate events in the parameter space $\Delta\phi$ (the angle between the $\not\!\!E_T$ and the nearest lepton or jet) vs $\not\!\!E_T$ (the missing transverse energy) as well as where one would expect top to lie. The background estimate for the dilepton channel is 2.1 ± 0.4 events[3]. Although not *a priori* part of the search, we examine the jets in dilepton events for indications that they originated from b-quarks. In the 10 dilepton events, we find 6 jets in 4 events (1 $\mu\mu$ and 3 $e\mu$) which

are identified ("tagged") as b-jets. This provides evidence for b-quarks produced in association with two W's, as expected from the decay of a $t\bar{t}$ pair.

CDF has also investigated top decays involving the τ-lepton. We have searched for dilepton events with one high-p_T electron or muon and one hadronically decaying τ-lepton which is identified using tracking and calorimeter quantities[7]. As in the $e\mu, ee$, or $\mu\mu$ channel two jets from b-quarks and significant missing transverse energy are required. Due to the additional undetectable τ-neutrino, the τ hadronic branching ratio and the lower efficiency for τ identification, the acceptance in this channel is considerably smaller than in the case of $e\mu, ee$, or $\mu\mu$. In 110 pb^{-1} we expect about 1 event from $t\bar{t}$ and 2 events from background. We observe 4 candidate events (2 $e\tau$ and 2 $\mu\tau$). There are 4 jets in 3 candidate events that are identified as b-jets ("tagged"). More data with excellent tracking will enable us to conclusively establish this "all 3^{rd} generation" decay mode of the top quark, which is important for charged Higgs searches and tests of weak universality.

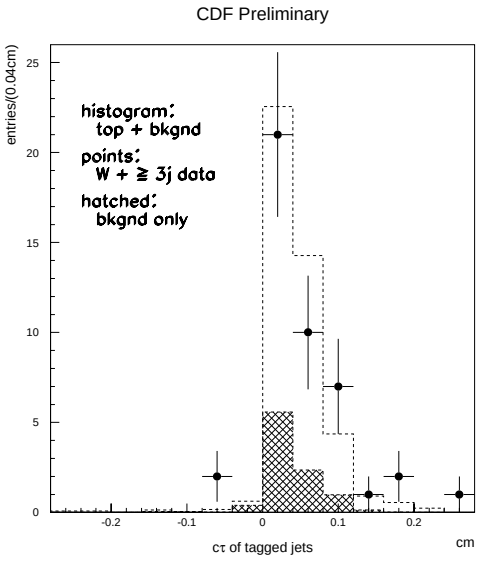

Figure 2.2: The proper time distribution for the b-tagged jets in the signal region (W+$\geq$ 3 jets). The open histogram shows the expected distribution of b's from 175 GeV/c^2 $t\bar{t}$ Monte Carlo simulation. The shaded histogram indicates the background in W+jet events.

2.2.1.2 Lepton + Jets Mode

In this channel, one of the W's decays leptonically to either an electron or muon (plus neutrino) and the other W decays hadronically to a pair of quarks. The nominal signature is a lepton, missing transverse energy (the neutrino from the leptonic W decay), and four jets; two from the b-quarks and two from the decay of the W. Approximately 30% of the $t\bar{t}$ events have this decay signature. Our lepton+jets selection requires that a leptonic W decay be accompanied by at least three central ($|\eta| < 2.0$) jets for an event to be considered part of the sample.

The background from W+multijet production is large. However, $t\bar{t}$ events contain two b-quark jets, and these can be distinguished from gluon and light quark jets in the background using two b-quark tagging techniques. The first technique locates a displaced vertex using the silicon-vertex detector (SVX Tag). The second locates a low-P_T electron or muon primarily from the semileptonic decay of a b-quark or sequential c-quark (SLT Tag). The efficiency for tagging a $t\bar{t}$ event is $(40 \pm 4)\%$ and $(20 \pm 3)\%$ for the SVX and SLT algorithms, respectively. In 110 pb^{-1}, 42 SVX tags are observed in 34 events. The background, in the 34 SVX tagged events, is estimated from a combination of data and Monte Carlo simulation to be 9.4 ± 1.4 events. Using the SLT tagging algorithm, 44 tags are found in 40 events. The background here is estimated to be 25.2 ± 3.8 events. The two samples have 11 events in common[3]. Figure 2.3 (upper left) shows the jet multiplicity spectrum for the SVX b-tags and the background.

In the 1 and 2-jet bins, we expect little contribution from $t\bar{t}$ events. The predicted background and the observed number of events agree well in the 1-jet bin, and agree at the 1.5 sigma level in the 2-jet bin as well. In the 3 and $\geq$4-jet bins, a clear excess of tagged events is observed. Fig. 2.2 shows the proper time distribution expected for b-tagged jets in the signal region ($\geq$ 3 jets), compared with that for the SVX b-tagged jets in the data: the tagged jets are consistent with b decays.

2.2.1.3 All Hadronic Mode

We have found a clear signal in the all-hadronic decay channel for $t\bar{t}$ events. In this decay mode there are six final state jets, four of which come from the hadronic decays of the two W's and two from the b-quarks. Approximately 44% of $t\bar{t}$ events have this decay signature. Achieving a reasonable signal-to-background ratio is the challenge in this data set

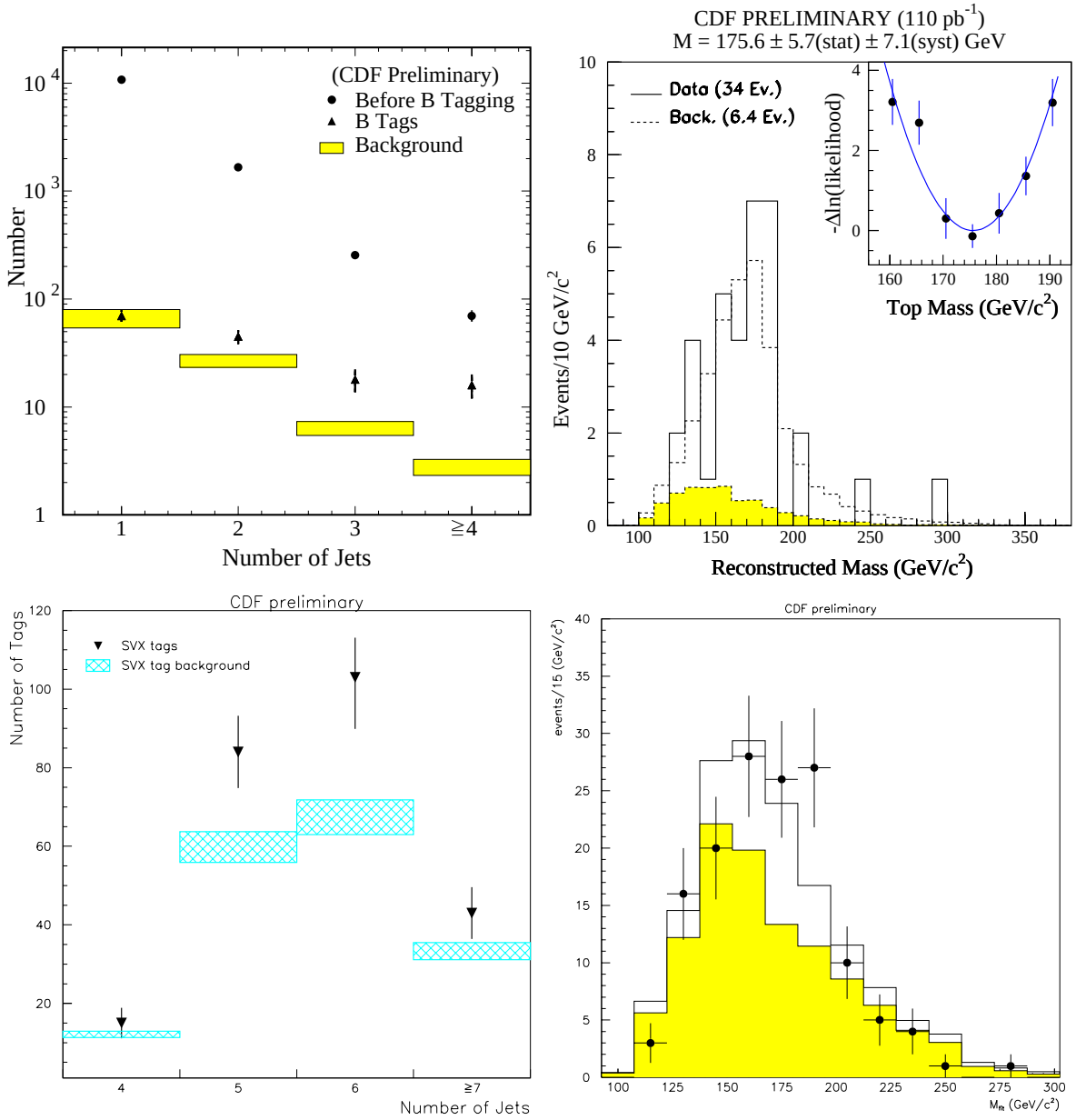

Figure 2.3: **Top Left:** The jet multiplicity distribution in SVX tagged W+jet events. Closed circles are number of events before b-tagging, dark triangles are number of b-tagged events in each bin and hatched areas are the background prediction for the number of tagged events and its uncertainty. **Top Right:** Mass spectrum for b-tagged lepton+jet events in 110 pb^{-1} of data. The shaded area is the expectation from background. The dashed curve is from background plus top production. The likelihood fit is shown as an inset. **Bottom Left:** The jet multiplicity distribution for the all-hadronic mode. The dark triangles represent the observed number of b-tags in each jet multiplicity bin and the hatched areas represent the background prediction as well as its estimated uncertainty. **Bottom Right:** Mass spectrum for all-hadronic b-tagged events in 110 pb^{-1} of data. The shaded area is the expectation from background. The histogram is from background plus top production.

which is dominated by QCD multijet production. In order to isolate a signal and maintain efficiency, we require at least five well-separated jets, one of which must be SVX b-tagged. After additional topological cuts, we find 230 tags in 192 events with an estimated background of 148 $\pm$ 10 events. Figure 2.3 (lower left) shows the jet multiplicity spectrum for the all-hadronic channel. In the 4-jet bin where we expect little contribution from $t\bar{t}$ events, the background and observed tags are in good agreement. Where we expect to see a signal for $t\bar{t}$, in the 5, 6, and $\geq$7-jet bins, an excess of tags is observed over the background predictions. [8]

2.2.1.4 Kinematic Discrimination

In addition to the search techniques based on the dileptons and b-quark tagging, CDF has isolated $t\bar{t}$ events based on the kinematical properties predicted from Monte Carlo simulations. These methods use the lepton+jets event sample but do not rely on b-tagging to reduce the background. One technique examines the jet E_T spectra of the second and third highest E_T jets [5]. The second technique uses the total transverse energy of the event [6]. In both cases, there is a clear $t\bar{t}$ component in our data.

2.2.1.5 $t\bar{t}$ Production Cross Section

The counting experiments which lead to a confirmed signal can be turned directly into measurements of the $t\bar{t}$ production rate. Figure 2.4 shows the $t\bar{t}$ production cross section measured in several channels in comparison to recent theoretical predictions. The best measurement to date is obtained from the weighted average of the counting experiments performed in the dilepton channel and the two lepton+jets channels, SVX b-tagging and SLT b-tagging. With 110 pb^{-1} of data, we measure a production cross section of $7.5^{+1.9}_{-1.6}$ pb[9, 10]. An independent measurement in the all-hadronic channel results in a cross section of 10.7 $^{+7.6}_{-4.0}$ pb [12]. A theoretical cross section calculation by Laenen *et al.* predicts 4.8 pb[17] at 176 GeV/c^2, and other recent theoretical cross sections are within approximately 15% of this value.[18, 19]

2.2.1.6 Top Quark Mass

The top quark mass has been measured in three different channels. The primary method is based on fully reconstructing the $t\bar{t}$ system with lepton+jets events. These events must contain a lepton and at least four jets such that each final state parton can be assigned to an observed jet or lepton. The reconstruction is performed using a constrained fitting technique which selects the best assignment of observed jets to final state partons based on the lowest χ^2. Without any b-tagging information there are 24 combinations which must be considered (12 parton assignments $\times$ 2 possible longitudinal momentum components for the neutrino). When one or two jets are tagged as b-quarks, the number of combinations is reduced to 12 and 4, respectively. The events containing at least one b-tagged jet provide the most precise mass measurement to date. Figure 2.3 (upper right) shows the reconstructed mass distribution for 34 events with at least one b-tag. The background estimate for this sample is $6.4^{+2.0}_{-1.5}$ events. Using a maximum likelihood technique, we determine a top quark mass of 175 ± 5.7 (stat.) $\pm$ 7.1 (syst.) GeV/c^2[3]. The systematic uncertainty is dominated by the uncertainty in final state gluon radiation, the b-tagging bias, and the detector energy scale.

The same constrained fitting technique was also used to reconstruct the top mass in the all-hadronic

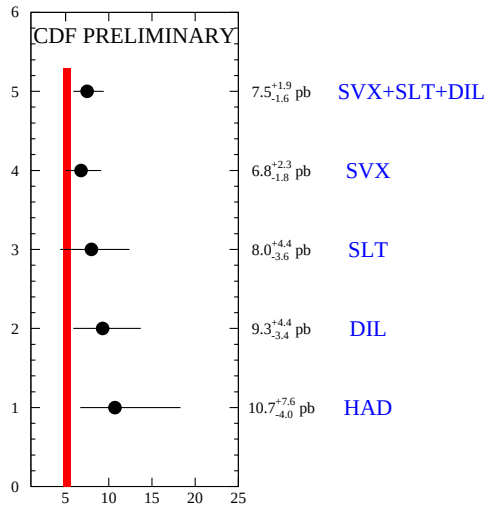

Figure 2.4: The measured cross section for $t\bar{t}$ production for each of the separate production channels measured at CDF as well as the combined lepton+jets and dilepton measurements. The vertical line represents the spread of the central values of the three most current theoretical calculations evaluated at a top mass of 175 GeV/c^2.

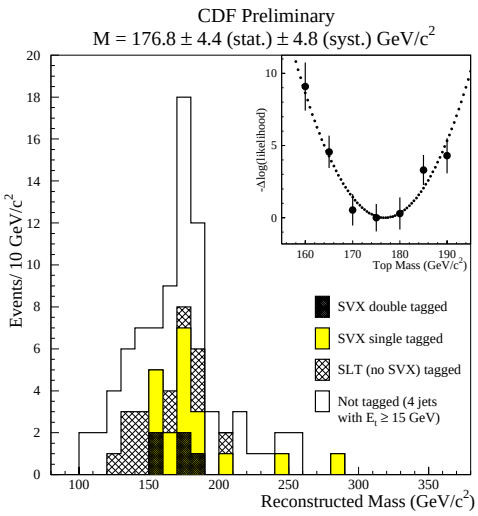

Figure 2.5: The optimized lepton+jets top quark mass plot for each of the four data samples. The insert shows the -Δlog(likelihood) for the data in comparison to mass spectra derived from Monte Carlo samples of various m_{top}. This technique results in a measured top quark mass of 176.8 ± 4.4 (stat.) ± 4.8 (syst.) GeV/c^2 – a 30% improvement over the old analysis.

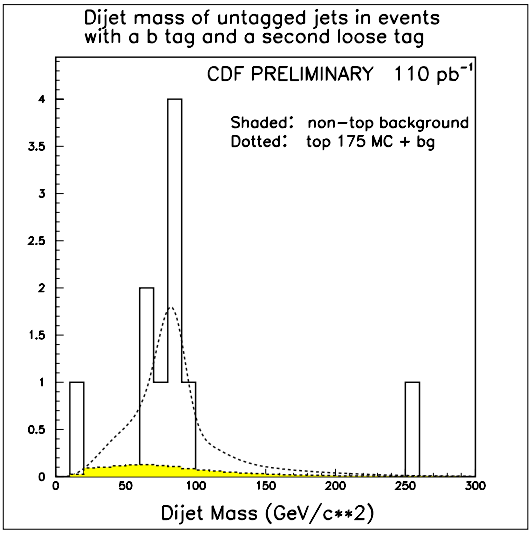

Figure 2.6: The M_{jj}^W distribution is shown for data (solid), expected top+background (dashed), and background (shaded), for W+4 jet events which contain two b-tagged jets. The value of M_{jj}^W is 79.8 $\pm$ 6.2 GeV/c^2. The top mass from this subsample has been determined to be 174.8 ± 9.7 GeV/c^2.

channel where at least one b-tag was required; the result is seen in Figure 2.3 (lower right). Applying a maximum likelihood technique to the data in this channel results in a top mass of 187 ± 8 (stat.) ± 12 (syst.) GeV/c^2.

A new optimization technique has recently been developed for determining the top quark mass in the lepton+jets mode [13]. The "original" method described above neglects information that is contained in the untagged sample, that is those events which satisfy all of our kinematic selection criteria but contain no b-tags. Moreover, the previous analysis combines the SLT and SVX data sets together, and information is lost because the signal-to-background ratio in those two channels is very different. The new optimized mass technique calculates the mass in four orthogonal data samples: the SVX single-tagged events, the SVX double-tagged events, the SLT tagged events which contain no SVX tags, and the not-tagged sample. The backgrounds are determined separately for each subset. The mass is then determined separately in each of these channels as described above and then combined by multiplying the individual mass likelihoods together. From this, one gets a top quark mass of 176.8 ± 4.4 (stat.) ± 4.8 (syst.) GeV/c^2 (see Figure 2.5). This optimization process reduces the total uncertainty on the top quark mass in the lepton + jets channel by 30%.

Reconstructing a top mass in the dilepton channel is difficult because this system is underconstrained. Instead, we measure the energy of the two b-jets and use a likelihood fit to compare the energy distribution in the data to Monte Carlo templates. This technique gives a top mass from dileptons of 156 ± 23 (stat.) ± 17 (syst.) GeV/c^2.

In the subsample of lepton+$\geq$ 4-jet events where two b-tags are required, we have looked for evidence of the decay of the hadronic W-boson. Fig. 2.6 shows the reconstructed mass of the unconstrained jet-jet system. A fit yields a jet-jet mass of 79.8 $\pm$ 6.2 GeV/c^2 [15]. This will be an important *in situ* technique for jet energy scale calibration in Run II. The top mass from this double b-tagged subsample has been determined to be 174.8 ± 8 (stat.) ± 6 (syst.) GeV/c^2.[14]

2.2.2 Lessons from Run I

- The detector should have the greatest possible acceptance for high-p_T electrons and muons from the chain $t \to W \to l\nu$.
- The detector should have the greatest possible acceptance and efficiency for tagging b-jets. This is a question of geometrical coverage, efficiency, and signal-to-noise ratio, most importantly for secondary vertex finding but also for soft lepton identification.
- Precision measurement of the top mass requires that the detector have *in situ* capability for understanding the systematics of jet energy calibration, including the ability to accumulate large samples triggered on low-p_T charged tracks, inclusive photons, and inclusive $W \to l\nu$ and $Z \to ll$.
- Understanding of b-tagging systematics has relied on the ability to accumulate a large, reasonably pure control sample of inclusive b-jets using low-p_T inclusive lepton triggers. We anticipate doing this again, with some demand on DAQ bandwidth. However, we have learned that jets containing $b \to cl\nu_l X$ are a biased control sample, and we believe that a large sample of b-jets collected with a secondary vertex trigger will be extremely useful.

2.2.3 Impact of Upgrades on Top Physics

The impact of the CDF II upgrades is to significantly increase the overall top acceptance and to maintain acceptance and precision at high luminosity.

- **Silicon Vertex Detector (SVX II)**: The tagging of b-quarks from top quark decay will be greatly improved in the long, 5-layer, double-sided device. Increasing the length of the silicon from 52 cm to 96 cm will extend the region of "contained b-jets" to cover the entire interaction region. With ten measurements in two views for any given track, it will be possible to make stringent track quality requirements, reducing the level of mistags, while still improving the overall track finding efficiency.

  A three-dimensional vertexing device will improve the b-tagging efficiency by making it possible to find b's whose displacement is predominantly in the Z direction. In addition, unlike a 2D vertex, a 3D vertex is unique with even 2 tracks, again raising the possibility of reducing backgrounds while increasing efficiency relative to the present analysis.

  Taking all of these factors into account, we anticipate that the SVX II will increase the efficiency for tagging at least one b-jet in a $t\bar{t}$ event to better than 65% (a 62% increase over the Run 1 efficiency), and will raise the double b-tag efficiency to 20% (a 200% increase from current performance) [23].

  Finally we point out that the 3D capability of the SVX II will allow a precision measurement of primary vertex in the event, improving a variety of measurements including the E_t/P_t of the primary leptons, the E_t of the jets, and the missing transverse energy.

- **Intermediate Silicon Layers (ISL)**: The ability to find unambiguous tracks pointing at the new plug calorimeter will provide clean identification of electrons from $W \to e\nu$ in the region $1.0 \leq |\eta| \leq 2.0$, improving the top yield in the electron channel by 33%. With the expected standalone tracking capability of the SVXII-ISL combination, b-tagging of top events will be possible out to $|\eta| = 2$, significantly improving the double-tagged top yield. The improved electron ID may also extend b-tagging with soft leptons into the plug region.

- **Central Outer Tracker (COT)**: The top analysis of Run I depended crucially on the large central tracking chamber. The new COT device will function better at the Run II luminosities than the current CTC did during Run I. It has more robust stereo tracking, lower mass, and better momentum resolution at the trigger level. As discussed in Chapter 7, the *integrated* system of COT-SVXII-ISL will bring much new power to bear on tracking at CDF II, and we are confident that we will exceed any performance estimate which is based on scaling from the Run I capabilities.

- **Plug Calorimeter Upgrade**: The new scintillating-tile fiber calorimeter with its shower max detector will provide improved jet resolution and electron identification in the forward region. The effect of improved electron identification is discussed above. The use of plug jets

Channel	Acc. A_{IB} (Run Ib)	Acc.,A_{II} (Run II)	Run I Results	Run II Yield (w/ A_{II})
Produced $t\bar{t}$	-	-	525	13.6k
Dileptons (ee,$\mu\mu$,$e\mu$)	0.78%	1.1%	10	155
Tau dileptons ($e\tau$, $\mu\tau$)	0.12%	0.14%	4	19
lepton+$\geq$3j	9.2%	11.2%	324	1520
lepton+$\geq$3j w/ $\geq$1 b tag	3.7%	7.3%	34	990
mass sample w/ $\geq$1 b SVX tag	3.0%	5.8%	20	790
mass sample w/ $\geq$2 b SVX tags	0.52%	1.8%	5	240

Table 2.2:
Acceptance and yield of $t\bar{t}$ events for a Run II upgraded detector. The yield is determined using the theoretical cross section (6.8 pb) at m_{top} = 175 GeV/c^2 and $\sqrt{s}$ = 2 TeV. For comparison, the acceptances for Run Ib are shown as well as the number of events seen in Run 1 prior to background subtraction. The acceptances include branching ratios and leptonic and kinematic selection (*e.g.* jet counting).

in a precision mass measurement will require ISL tracking in order that the *in situ* jet energy calibrations established for the central calorimeter can be extended to the plug region.

- **Muon Detection System**: The more complete ϕ and η coverage will assist in the identification of primary muons from W decay and low-P_T muons from semileptonic b-quark decay. The closure of the gaps in the muon system will increase the total muon acceptance for top by 12%. Equally important but difficult to quantify at this point in time is the impact these changes will have on the muon trigger rates. The additions to the CMP increase its total physical coverage by 30% [23], but since the CMP is a confirmation layer behind the CMU, the effect will be on rates rather than acceptance. We expect a much simplified set of muon triggers and trigger systematics, with implications for measurement of the $t\bar{t}$ cross section, and we also expect a much purer sample of b-jets where $b \rightarrow \mu\nu X$ jets for the study of b-tagging systematics.

2.2.4 Event Yield

To estimate the yield of top events, we extrapolate from our current measured acceptance using the theoretical cross section (6.8 pb) at m_{top} = 175 GeV/c^2 and $\sqrt{s}$ = 2 TeV [22, 11].

At $\sqrt{s}$ =2 TeV, the $t\bar{t}$ cross section is approximately 40% higher than at $\sqrt{s}$=1.8 TeV. We assume that the additional lepton and b-tagging acceptance outlined in Sec. 2.2.3 above can be incorporated while maintaining a signal-to-background ratio comparable to the Run I analysis.

Table 2.2 summarizes the acceptance and yields for various decay channels in the Run II configuration. The Run Ib acceptances are shown for comparison. A sample of 2 fb^{-1} at the Tevatron will provide over 1000 identified b-tagged $t\bar{t}$ events.

2.2.5 Measurement of the Top Quark Mass

The top quark mass will be one of the most important electroweak measurements made at the Tevatron. In combination with the W mass, m_t gives information about the mass of the standard model Higgs boson. The precision electroweak program and the W mass measurement are discussed in the electro-weak section of Chapter 2. Figure 2.13 shows how the predicted top and W mass measurements constrain the Higgs mass. In that figure, the uncertainty on the top mass is taken as 4 GeV/c^2.

Currently, the statistical and systematic uncertainties on CDF's top mass measurement are both about 5 GeV. The statistical uncertainty should scale as $1/\sqrt{N}$. Using the yields in Table 2.2, we anticipate that the statistical uncertainty on the top mass in the optimized lepton+$\geq$ 4-jet sample with at least one b-tagged jet will be $\approx$ 1 GeV/c^2. We see that in Run II the uncertainty will be dominated by systematics.

Note that with the new integrated tracking, the acceptance for double-tagged lepton+$\geq$ 4-jet events increases by about a factor of 2.5. In these double-tagged events, the number of unique combinations for the constrained mass fitter to test is 4 instead of 12, improving the mass resolution by 20%. Thus, using only double-tagged events, CDF II can still achieve a statistical uncertainty which approaches 1 GeV/c^2. Because both b-quarks are identified in double-tagged events, the systematics ultimately may be better understood for this class of events.

Almost all of the systematic uncertainties in the top mass measurement are coupled to the reliability of the Monte Carlo models for the spectrum of fit masses in signal and background. Assuming the theory model is accurate, most of the uncertainty is related to resolution effects. Instrumental contributions include calorimeter nonlinearity, losses in cracks, dead zones, and absolute energy scale. A larger and more difficult part of the energy resolution concerns the reliability of the extrapolation to parton energies. Ultimately, it may be our understanding of QCD and not the detector which limits the mass resolution.

Many of these issues can be addressed by *in situ* calibration procedures. For example, Z+jet events are used to understand the systematic uncertainty due to energy scale and gluon radiation, two of the dominant uncertainties. In 2 fb^{-1}, we expect to have 27K (70) Z's with 1 (4) or more jets. The effect of gluon radiation will also be studied in large statistics samples of W+jets, γ+jets, and $b\bar{b}$ events. In addition, the mass peak from $W \rightarrow qq'$ (see Figure 2.6) in the lepton + jets top sample allows an energy scale calibration *in exactly the same events and environment* as the mass measurement. A complete model study of the extrapolation of the systematic uncertainty on the top mass can be found in Ref. [1].

In any case, if all systematic effects can be measured or otherwise connected with mean quantities in large statistics control samples, the systematic uncertainties should also scale as $1/\sqrt{\mathcal{L}}$. We can conservatively assume in this case that we can reduce our systematic error to $\approx$ 2 GeV/c^2. This is probably our lower limit. We use 3 GeV/c^2 as our goal for the total uncertainty on the top quark mass.

2.2.6 Production Cross Section, $\sigma_{t\bar{t}}$

An accurate measurement of the $t\bar{t}$ production cross section is a precision test of QCD. A cross section which is significantly higher than the theoretical expectation would be a sign of non-standard model production mechanisms, for example the decay of a heavy resonant state into $t\bar{t}$ pairs or anomalous couplings in QCD. As in the case of the top mass, large statistics in the lepton+jets mode imply that systematic uncertainties will be the limiting factor in the cross section measurement.

For the acceptance, the reliability of jet counting and b-tagging are at issue. Initial state radiation can be examined using a sample of Z+jets, while the jet energy threshold uncertainty can be addressed as in the top mass discussion. With 2 fb^{-1} of data it will be possible to measure the b-tagging efficiency *in top events*, using dilepton events selected without a b-tag and the ratio of single to double tags in lepton+jets events. We assume that these studies will give uncertainties that scale with $\sqrt{N}$.

With large samples, one can measure the bottom and charm content as a function of jet multiplicity in W + jet events using the cτ distribution of the tagged jets and use this to tune the Monte Carlo models for W+$\geq$ 3-jet backgrounds. Finally, in Run II and beyond, the luminosity will be measured either through the $W \rightarrow l\nu$ rate, or the mean number of interactions per crossing, and we will assume 5% for the future precision of the luminosity normalization.

Accounting for all effects we find that the total $t\bar{t}$ cross section can be measured with a precision of 9% for 2 fb^{-1}. This will challenge QCD, and provide a sensitive test for non-standard production and decay mechanisms.

2.2.6.1 Measurement of a t $\rightarrow$ W Branching Fraction

The ratio of the $t\bar{t}$ cross section measured using dilepton events to that measured using lepton+jets events is a test for non-standard model decay modes of the top quark. Since the cross section in each case assumes that each top decays into W-bosons, a ratio different from 1.0 would signal decays *without* a W-boson, such as charged Higgs (t $\rightarrow$ H$^+$ b) or light supersymmetric top (stop). The reach for a particular non-standard decay is model dependent, but we can say that with 2 fb^{-1} of data, we will be able to measure the basic dilepton to lepton+jets ratio to 12%,

and the top branching fraction to W in association with b with a precision of 9%.

2.2.7 Measurement of a t → b Branching Fraction and a Lower Limit on V_{tb}

In the standard model with 3 generations, existing experimental constraints and the unitarity of the CKM matrix require $V_{tb} \simeq 1$, predicting that the weak decay of the top will proceed almost exclusively through W + b. In events containing a W, the top branching fraction to b's is related to the CKM element according to:

$$\begin{aligned} B_b &= B(t \to W(b)) \\ &= \frac{\sigma(t \to Wb)}{\sigma(t \to Wq)} \\ &= \frac{|V_{tb}|^2}{|V_{td}|^2 + |V_{ts}|^2 + |V_{tb}|^2} \end{aligned}$$

The notation above is meant to indicate that a W has been required in the final state, and this is not the decay fraction to W+b, but the fraction of decays with W's which *also* contain b's. Since the standard analysis identifies $t\bar{t}$ events by requiring at least 1 W and 1 b, $B(t \to W(b))$ is measured from the number and distribution of tagged b-jets in top events. Four different techniques can be used to measure this distribution: [20, 21]

- The ratio of double b-tagged to single b-tagged events in the b-tagged lepton+jets sample: requiring one b-jet to be tagged leaves the second jet unbiased, and from a known tagging efficiency, one can extract the branching ratio from the ratio of tagged to untagged "second jets". [20]
- The ratio of single b-tagged to no b-tagged events in a lepton+jets sample in which kinematic criteria have been applied: since there is no a-priori tag requirement, we can extract the branching ratio from the ratio of single tagged events to not-tagged events. An ideal sample for this is the W+4 jet mass sample prior to applying the χ^2 cut. [21]
- The number of b-tagged jets in the dilepton sample: Since b-tagging is not required to identify tops decaying to dileptons, the whole b-tag multiplicity distribution in these events contains information on $B(t \to W(b))$. Despite the smaller branching fraction to dileptons, the statistical powers of the dilepton and lepton+jets samples are comparable.
- The distribution of double tags: If there are two tagging algorithms (soft leptons and secondary vertex), one can compare the number of times that events tagged by both algorithms have both tags in the same jet vs. the number of times the tags are in different jets. Small values of $B(t \to Wb)/B(t \to Wq)$ result in large values of the same to different jet ratio.

These techniques are not exclusive, and can be combined. We have used a maximum likelihood estimator to do this combination in Run I data. With 100 pb^{-1}, CDF has a ±25% statistical uncertainty on the branching fraction, but only an ±11% systematic uncertainty. The systematic uncertainty is dominated by the uncertainty on the tagging efficiency, which is measured in the data using b-rich inclusive lepton samples. This uncertainty should fall as $1/\sqrt{N}$. The small non-$t\bar{t}$ backgrounds will be measured to high accuracy by Run II. For Run II, we expect to measure $B(t \to W(b))$ to 3.0% and place a 95% CL lower limit of 0.25 on $|V_{tb}|$.

2.2.7.1 Anomalous Couplings and Weak Universality

Since the top quark is so heavy, it is possible that the physics of the underlying theory may manifest itself via new non-universal top interactions. The top quark is unique in that it decays prior to hadronization and therefore the decay products carry helicity information related to the fundamental couplings. In the standard model, the top quark decays only to longitudinal or left-handed W's, where the ratio is given by

$$\frac{W_{long}}{W_{left}} = \frac{1}{2}\left(\frac{m_{top}}{m_W}\right)^2$$

For $m_{top} = 170$ GeV/c^2, the branching fraction to longitudinal W's is 69.2%. In many cases non-universal top couplings will appear as a departure of B($t \to bW_{\rm long}$) from the standard value and we use this quantity as our precision benchmark for probes of anomalous weak couplings.

Experimentally, we have access to the polarization state of the decay W through the charged lepton helicity angle, $cos\theta^*_e$ which can be measured in the lab

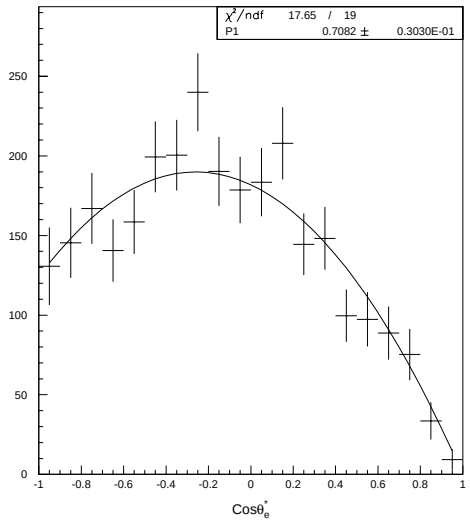

Figure 2.7: The $\cos\theta_e^*$ distribution for 1000 events and fit to the standard model hypothesis $\sim 30\%$ $W_{\rm left} + 70\%$ $W_{\rm long}$

frame as

$$\cos\theta_e^* \approx \frac{2M_{eb}^2}{m_{e\bar{b}\nu}^2 - M_W^2} - 1 \qquad (2.1)$$

The resulting distribution can then be fit to a superposition of W helicity amplitudes in order to measure any possible contribution of non-universal weak couplings in the top decay.

Our model study uses a four-vector level Monte Carlo [16] with selection bias and resolution smearing modeled on the CDF experience. We assume the constrained mass fit will allow us to know perfectly which b-jet belongs to the semi-leptonic top decay. This is clearly optimistic. We correct the $\cos\theta_e^*$ distribution for the bias imposed by the selection cuts. This acceptance corrected distribution for 1000 events is shown as the data points in Fig. 2.7. We fit the distribution to the standard model hypothesis for the admixture of $W_{\rm long}$ and $W_{\rm left}$ and get a good fit with $\mathrm{B}(t \to bW_{\rm long}) = 0.708 \pm 0.030$, as shown.

We have estimated the systematic uncertainty from W-b combinatorics, energy scale uncertainties, and backgrounds. We find that with 2 fb^{-1}the top quark decay branching fraction to longitudinal W-bosons can be measured with a total precision approaching 5%. We have also studied the effect of a V+A term in top decay and find similar sensitivity.

2.2.7.2 Single Top Quark Production

In addition to $t\bar{t}$ pair production via the strong interactions, top quarks can also be produced singly via the electroweak interaction. This process depends on the t-W-b vertex, and the production rate is a measure of the top decay width to W+b and the CKM matrix element $|V_{tb}|^2$.

The two dominant single top processes at the Tevatron are the s-channel mechanism $qq \to t\bar{b}$, referred to here as W^* production, and the t-channel interaction $qb \to qt$, referred to as W-gluon fusion. Other processes become important at higher energies, but are negligible here. The W-gluon fusion process is thought to dominate the production with an estimated cross section of 1.44 pb; the uncertainties on this calculation are large – on the order of 30%. The W^* production mode has an estimated cross section of 0.74 pb with an uncertainty of 6%. The combined rate for single top production by these two processes is ≈ 2.2 pb, only a factor of 3.5 down from the $t\bar{t}$ rate at this energy.

The TeV-2000 group studied single top production using the ONETOP Monte Carlo with $m_t = 170$ GeV/c^2 [16]. The detector performance for b-tagging was based on the CDF Run Ib result, as was the size of the b-tagging backgrounds. The jet energies were smeared according to the resolution model $(82\%/\sqrt{E} + 18\%)$, which is very conservative compared to the CDF II goal of $\sigma_{E_T} = 0.1 \cdot E_T + 1$ GeV.

The data selection criteria that were used to isolate the signal over background include:

- Exactly two jets with $E_T > 20$ GeV, $|\eta|_{\rm jets} < 2.5$
- $\Delta R = \sqrt{(\Delta\phi)^2 + (\Delta\eta)^2} > 0.5$ between all jet pairs and jet-electron pairs
- $\not\!\!E_T > 20$ GeV
- $E_T(\text{electron}) > 20$ GeV
- $|\eta|_{\rm electron} < 2.5$
- No second isolated electron present with $E_T > 20$ GeV
- At least one jet tagged as a b-jet.

The signal for single top production is a peak in the Wb invariant mass plot. The shape of the signal-plus-background curve is easily distinguished from the background shape alone using the conservative

resolution. The size of signal (S) and background (B) are counted using the number of events in a mass peak window of 50 GeV/c^2 around the generated top quark mass: there is a signal yield of approximately 100 events per fb^{-1}, above a background about twice as large, mainly from W + $b\bar{b}$. Assuming that the background normalization is understood (through the large statistics top cross section measurement), the statistical precision on the single top cross section using 2 fb^{-1} will be about 12%.

Many of the sources of systematic uncertainty in the single top cross section are common to the $t\bar{t}$ cross section discussed earlier. We assume that systematic uncertainties related to selection efficiencies and backgrounds will shrink as $\sqrt{N}$. For the case of 2 fb^{-1} we find that the measurement of the single top cross section will have a total uncertainty of approximately 24%.

The single top cross section is directly proportional to the partial width , ($t \to Wb$) and assuming there are no anomalous couplings, this is a direct measure of $|V_{tb}|^2$. There are theoretical uncertainties in converting the cross section to the width, notably for the gluon fusion process. Taking these into account, we anticipate that a measurement of the total single top rate with 2 fb^{-1} will translate in a precision of 26% on , ($t \to Wb$) and 13% on $|V_{tb}|$.

The theoretical determination of W* is more reliable than that of W-gluon fusion since initial state effects can be measured in the similar Drell-Yan process, and if the data set is large enough this may afford the best precision on the width. The two processes can be separated by requiring two b-tags since the double tag rate for W* production is close to a factor of 5 more than that of W-gluon fusion.

2.2.8 Search for Anomalously Large Rare Decays

- $t \to Zc, \gamma c$
- $t \to WZb$
- $t \to W^+W^-c$
- $t \to Hc$

The standard model predicts that the branching fractions of FCNC top decays are around 10^{-10} [29], out of reach for even the LHC. Any observation of such decays will signal new physics. As illustration, we consider the signal for a flavor changing neutral current decay $t \to c\gamma$ in a $t\bar{t}$ event. If the other top in the event decays in the leptonic channel, the acceptance is almost the same as the standard model lepton+jets mode, and it then becomes a simple matter to scale from present results. The background from $W + \gamma$ + two jets is about 1 fb. Although it is unlikely that this background will be kinematically consistent with $t\bar{t}$ (for example, that $m(\gamma + j) = m(t)$), we take the very conservative assumption that this background is irreducible. We find that 2 fb^{-1} will probe branching fractions for this decay down to 3.0×10^{-3}

Sensitivity to other rare decays can be scaled from this estimate. For the case $t \to Z + c$, where the Z decays to leptons, after adjusting for branching ratios and different backgrounds, we find sensitivity down to 1.5%.

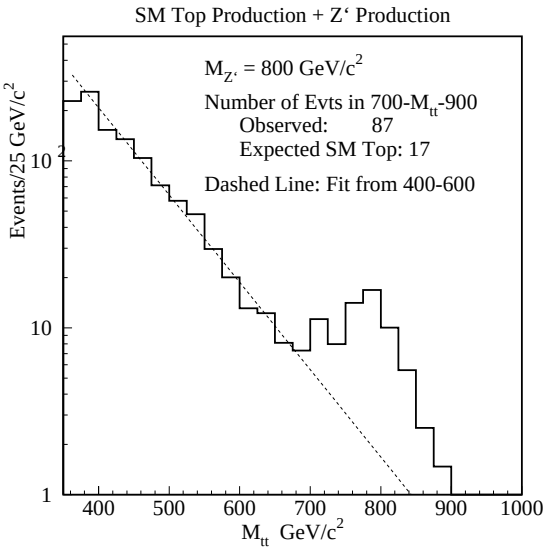

Figure 2.8: A hypothetical $m_{t\bar{t}}$ spectrum with an 800 GeV/c^2 Z′ topcolor boson. The rate is based on the theoretical predicted cross section for $t\bar{t}$ production and Z′ production [31] with 2 fb^{-1}.

2.2.8.1 Dynamical Symmetry Breaking

Because of its large mass, the top quark is an excellent probe for physics beyond the standard model. Theories which implicate top in the electroweak symmetry breaking mechanism, such as a color-octet vector meson associated with a top condensate[33] or multiscale technicolor[34], predict enhancements or changes in the shape of the $t\bar{t}$ invariant mass spectrum ($m_{t\bar{t}}$) and the top quark transverse momentum

Measurement	2 fb^{-1}	Comment
Yields		
N_{3jet*b}	990	*identified* events
$N_{4jet*2b}$	240	clean m_t sample
δm_t	3	total precision GeV/c^2
Production		
$\delta\sigma_{t\bar{t}}$	9%	test top QCD couplings
$\delta\sigma_{ll}/\sigma_{l+j}$	12%	test non W decay
$\delta\sigma_{t\bar{b}X+b\bar{t}X}$	24%	isolate "single top"
$\delta\sigma \cdot B(Z' \to t\bar{t})$	90 fb	"topcolor" $M_{Z'}$ = 1 TeV/c^2
Decay		
$\delta B(t \to W(b))$	2.8%	from N(bb)/N(bX)
$\delta B(t \to b(W))$	9%	from N(ll)/N(lX)
$\delta B(W_{V+A})$	2.7%	$W \to l\,\nu$ helicity
$\delta B(W_{long})$	5.5%	$\frac{W_{long}}{W_{left}} = \frac{1}{2}(\frac{m_{top}}{m_W})^2$
δ, $(t \to Wb)$	26%	using single top
δV_{tb}	13%	from above
Rare Decays		
B(c γ)	$\leq 2.8 \times 10^{-3}$	(95% CL)
B(cZ)	$\leq 1.3 \times 10^{-2}$	(95% CL)
B(Hb)	$\leq$ 12%	from σ_{ll}/σ_{l+j}

Table 2.3: Summary of expected measurement accuracies for an integrated luminosity of 2 fb^{-1}

distribution (P_T^{top}).

CDF is currently searching for resonances, $X \to t\bar{t}$, in the $M_{t\bar{t}}$ spectrum by reconstructing $M_{t\bar{t}}$ on an event-by-event basis using the same event sample and constrained fitting techniques used in the top mass measurement, with an additional constraint that the t and $\bar{t}$ decay products have a mass equal to the measured m_{top}. By the end of Run I, we should have sensitivity to new objects with masses as large as 500-600 GeV/c^2. In the absence of a signal, limits in Run II will be as high as 1000 GeV/c^2. New resonances with masses below the limit could be observed. For example, Figure 2.8 shows the $M_{t\bar{t}}$ spectrum for 2 fb^{-1} with standard model $t\bar{t}$ production plus the addition of a topcolor Z′ at 800 GeV/c^2 [31], where the Z′ decays to a $t\bar{t}$ pair. In this theory, the branching fraction of Z′ to $t\bar{t}$ pairs is potentially large (50-80%) but depends on the Z′ width. In the case shown in Figure 2.8, we would expect 17 events from standard model $t\bar{t}$ production in the range $700 < M_{t\bar{t}} < 900$ GeV/c^2 and 70 events from $Z' \to t\bar{t}$ in this range. The $M_{t\bar{t}}$ spectrum along with other $t\bar{t}$ production distributions provide an excellent means for searching for new phenomena.

2.2.9 Summary of Top Physics

For the next decade, the Tevatron will be the only accelerator capable of producing the top quark, and an upgraded CDF II detector will be well-suited for the study of top physics. The increased coverage of the SVX II detector and muon systems will allow us to tag at least one b-quark in $\approx$ 65% of $t\bar{t}$ events and both b-quarks in 20% of the events. With 2 fb^{-1} of integrated luminosity, we expect 1000 single SVX-tagged $t\bar{t}$ events in the lepton+jets channel.

The top physics program possible with this sample is summarized in Table 2.3. We expect to measure the top mass, a fundamental electroweak parameter, with a precision of approximately 3 GeV/c^2. Measurements of branching ratios, angular distributions, and top production mechanisms with the sensitivities listed in Table 2.3 will provide the first complete

characterization of this new fermion. Our catalog of possible measurements is hardly complete. But in the event that the top quark yields surprises, these sensitivities benchmark the capability to explore new physics at the Fermilab Tevatron.

Bibliography

[1] *Future ElectroWeak Physics at the Fermilab Tevatron: Report of the TeV_2000 Study Group*, Editors D. Amidei and R. Brock Fermilab–Pub–96/082

[2] F. Abe *et al.* (CDF Collaboration), Phys. Rev. D **50**, 2966 (1994); F. Abe *et. al.* (CDF Collaboration), Phys. Rev. Lett. **73**, 225 (1994).

[3] F. Abe *et al.* (CDF Collaboration), Phys. Rev. Lett. **74**, 2626 (1995).

[4] S. Abachi *et al.* (D0 Collaboration), Phys. Rev. Lett. **74**, 2632 (1995).

[5] F. Abe *et al.* (CDF Collaboration), Phys. Rev. D **52**, R2605 (1995).

[6] F. Abe *et al.* (CDF collaboration), Phys. Rev. Lett. **75**, 3997 (1995).

[7] M. Hohlmann, *Observation of Top quarks in the dilepton decay channel* $t\bar{t} \rightarrow e(\mu)\nu_{e(\mu)}\ \tau\nu_\tau\ b\bar{b}$ *Using Hadronic Tau Decays At CDF*, Proc., Lake Louise Winter Institute (1996)

[8] P. Azzi *et al.*, *Hadronic Top Production at CDF*, CDF Note 3679.

[9] R. Hughes, B. Winer, T. Liss, *Combining the SVX, SLT, and Dilepton* $t\bar{t}$ *Cross Sections*, CDF Note 3111.

[10] T. Liss, R. Roser, $t\bar{t}$ *Production Cross Section for 110* pb^{-1}, CDF Note 3481.

[11] A. Beretvas, Int. J. Mod. Phys. A11, 2045 (1996)

[12] P. Azzi *et al.*, $t\bar{t}$ *Production Cross Section in the All-hadronic Channel*, CDF Note 3464.

[13] K. Tollefson *et al.*, *Optimizing the Top Quark Mass Measurement*, CDF Note 3606.

[14] S. Aota *et al.*, *Update to Top Mass on Double b-tagged Events Using Loose Jet Probability Tagging*, CDF Note 3604.

[15] R. Wilkinson *et al.*, *Update to Hadronic W Decays in Double b tagged Top Candidates*, CDF Note 3543.

[16] E. Malkawi, C.-P. Yuan, *A Global Analysis of the Top Quark Couplings to Gauge Bosons*, Phys. Rev. D **50**, R4462 (1994).

[17] E. Laenen, J. Smith, W.L. van Neerven, Phys. Lett. **321B**, 254 (1994).

[18] Catani, Mangano, Nason and Trentadue, CERN Preprint, CERN-TH/96-21 hep-ph/9602208.

[19] E. Berger, Argonne Nat. Lab. Preprint ANL-HEP-PR-95-31

[20] T. LeCompte, R. Roser, *Measurement of* $BF(t \rightarrow Wb)$ *and the CKM Matrix Element* $|V_{tb}|$ *in Top Decays*, CDF Note 3056.

[21] F. Bedeschi, G. Chiarelli, F. Tartarelli, *Measurement of* $BF(t \rightarrow Wb)$ *in Top Decays*, CDF Note 3853.

[22] E. Laenen, private communication.

[23] R. Hughes, R. Roser, from a series of talks at the CDF upgrade meetings

[24] D. Atwood, A. Kagan, T.G. Rizzo, *Constraining Anomalous Top Quark Couplings at the Tevatron*, SLAC-PUB-6580, July 1994.

[25] G. Kane, C.-P. Yuan, and D. Ladinsky, Phys. Rev. D **45**, 124, (1992); D. Atwood, A. Aeppli, and A. Soni, Phys. Rev. Lett. **69**, 2754, (1992); R.S. Chivukula, S.B. Selipsky, E.H. Simmons, Phys. Rev. Lett. **69**, 575, (1992); M.Peskin, talk presented at the *Second International Workshop on Physics and Experiments at a Linear e+e- Collider*, Waikoloa, HI, April 1993; M.Peskin and P. Zerwas, talks presented at the *First International Workshop on Physics and Experiments at a Linear e+e- Collider*, Saariselka, Finland, September 1991.

[26] S. Dawson, Nucl. Phys. **B249**, 42 (1985); S.S.D. Willenbrock and D.A. Dicus, Phys. Rev. D **34**, 155 (1986); S. Dawson and S.S.D. Willenbrock, Nucl. Phys. **B284**, 449 (1987); C.-P. Yuan, Phys. Rev. D **41**, 42 (1990); S. Cortese and R. Petronzio, Phys. Lett. **B253**, 494 (1991); G.V. Jikia and S.R. Slabospitsky, Phys. Lett **B295**, 136 (1992), R.K. Ellis and S. Parke, Phys. Rev. D **46**, 3785 (1992); G. Bordes and B. van Eijk, Z. Phys. **C57**, 81 (1993); G. Bordes and B. van Eijk, Nucl. Phys. **B435**, 23 (1995): T. Stelzer and S. Willenbrock, Phys. Lett. **B357**, 125-130 (1995).

[27] D. Winn, D. Amidei, *Study of the $t \to Wb$ Vertex at CDF*, CDF Note 2914.

[28] D.O.Carlson, C.-P. Yuan, Phys. Lett. **306B**, 386 (1993).

[29] S. Parke, *Summary of Top Quark Physics*, FERMILAB -Conf-94/322-T. Presented at DPF'94, University of New Mexico, Albuquerque, NM, August 2-6, 1994.

[30] T. Stelzer, S. Willenbrock, *Single-Top-Quark Production via $q\bar{q} \to t\bar{b}$*, DTP/95/40, ILL-(TH)-95-30 (1995).

[31] C. Hill, *Topcolor Assisted Technicolor*, Fermilab-Pub-94/395-T

[32] K. Lane, *Top Quarks and Flavor Physics*, BUHEP–95–2.

[33] C. T. Hill, Physics Lett. **266B**, 419 (1991).

[34] K. Lane, E. Eichten, Phys. Lett. **222B**, 274 (1989); K. Lane and M.V. Ramana, Phys. Rev. D **44**, 2678, (1991).